Nuclear Instruments and Methods in Physics Research A 704 (2013) 19–26

Contents lists available at SciVerse ScienceDirect

Nuclear Instruments and Methods in Physics Research A

journal homepage: www.elsevier.com/locate/nima

$LaBr_3(Ce)$:$LaCl_3(Ce)$ Phoswich with pulse shape analysis for high energy gamma-ray and proton identification

O. Tengblad [a,*], T. Nilsson [b], E. Nácher [a], H.T. Johansson [b], J.A. Briz [a], M. Carmona-Gallardo [a], C. Cruz [a], V. Gugliermina [a], A. Perea [a], J. Sanchez del Rio [a], M. Turrión Nieves [a], J. Bergström [b], E. Blomberg [b], A. Bülling [b], E. Gallneby [b], J. Hagdahl [b], L. Jansson [b], K. Jareteg [b], R. Masgren [b], M. Nordström [b], G. Risting [b], S. Shojaee [b], H. Wittler [b]

[a] Instituto de Estructura de la Materia, CSIC, E-28006 Madrid, Spain
[b] Department of Fundamental Physics, Chalmers University of Technology, S-41296 Göteborg, Sweden

ARTICLE INFO

Article history:
Received 23 May 2012
Received in revised form
13 November 2012
Accepted 16 November 2012
Available online 29 November 2012

Keywords:
Phoswich scintillator
Gamma calorimeter
$LaBr_3(Ce)$
$LaCl_3(Ce)$
Pulse shape analysis

ABSTRACT

A novel Phoswich design based on new generation scintillator crystals is presented. The detector composed from a combination of a $LaBr_3(Ce)$ with a $LaCl_3(Ce)$ crystal in one cylinder coupled to a photo multiplier tube has been tested both for incident gamma rays in the range of 0.3–6 MeV, as well as for high energy protons in the range 120–180 MeV. The Phoswich assembly has not significantly deteriorated the energy resolution, which for 662 KeV gamma rays gives a resolution of 4.5%, while for high energy protons (E_p = 180 MeV) an energy resolution of 1% was obtained. It is shown that the signals from the two crystals can be separated in an *event by event* based mode. Using direct digitizing of the detector pulse an off-line pulse-shape analysis was performed built either on a *total to tail* or *total to pulse height* method in order to fully identify the incoming radiation. Our aim with this R&D is to in the future build a detector which is able to detect with good efficiency and resolution over a wide energy range; 0.1–30 MeV gamma rays and 20–400 MeV protons. Monte Carlo simulations made in order to design the next prototype are presented.

1. Introduction

During the past decade it has been demonstrated that reactions with exotic secondary beams are an important tool for exploring the properties of nuclei far from stability, and allow for detailed spectroscopic information to be extracted. The physics motivation for studying reactions with exotic nuclei is described extensively in various reports in the context of next-generation facilities, see e.g. the 'Conceptual Design Report' (CDR) [1] for the future FAIR project or the one for SPIRAL2 [2].

As gamma-ray detection constitutes an important experimental probe common to all these physics topics, the powerful future accelerator facilities require a new generation of gamma detector arrays capable of exploiting the full potential of these highly exotic and/or high intensity beams.

In many cases the spectrometer should be able to measure the total energy of the gamma cascade, the multiplicity and the individual energies of each gamma-ray with great efficiency and high energy resolution. Further, in many cases the spectrometer should also be able to detect and determine the energy of high energy protons. The requirements of the crystals to detect protons and gamma-rays are, in first approximation, quite different, but we will present a method that can be adapted to both cases.

In nuclear reaction experiments at very high (relativistic) energies the gamma rays emitted in flight will suffer Doppler broadening, further the kinematics implies greater energy correction (Lorentz transformation) at smaller emission angles and thus a special solution is needed for the detection in the forward direction. Here we are presenting a novel method using crystals of new generation and detectors formed by two layers of crystals with a single readout, the so called Phoswich detectors.

2. Phoswich approach

Due to the high beam energy used in many reaction experiments e.g. at R3B@FAIR [3], the Lorentz boost applied to the in-flight emitted gamma-rays will be such that a 10 MeV gamma-ray energy will be shifted to 20 or even 30 MeV depending upon the emission angle. At such a high energy, the interaction of gamma-rays with matter is dominated by pair production. Monte Carlo simulations show that, about half of the gamma-rays of 20 MeV

* Corresponding author. Tel: +34 915616800/943002; fax: +34 915855413.
E-mail address: olof.tengblad@csic.es (O. Tengblad).

0168-9002/$ - see front matter © 2012 Elsevier B.V. All rights reserved.
http://dx.doi.org/10.1016/j.nima.2012.11.094

suffer from pair production within the first 5 cm of a $LaBr_3(Ce)$ crystal, depositing most of their energy in and around the first interaction. Having two layers of different crystals and being able to distinguish between the energy deposited in both, will allow us to implement intelligent add-back algorithms in which, by imposing conditions on one or the other layer (veto or coincidence), one can obtain information about the physical processes and even reconstruct part of the energy lost.

Protons, contrary to gamma-rays, interact in a material by a continuous slow down, leaving part of their energy along the track, but they will deposit most of their energy in the final absorption process (Bragg peak). This also favors the use of two layers. Instead of using one very long crystal (25–30 cm); it is possible to determine the initial energy from the energy loss in two shorter crystals, and thus avoid the Bragg peak of very high energy protons (>200 MeV) where a major part of the energy might escape due to the production of neutral particles (pions or neutrons).

In the choice of scintillator material to be used in a Phoswich configuration one has to take into account that the crystals must be optically compatible i.e. the second layer crystal has to be transparent to the light emitted by the first layer. A Phoswich solution coupling LSO and LYSO (see e.g. Ref. [4]) has already been tested. However, the energy resolution for the LSO and LYSO crystals are though in the range of 9–12% [4] for 662 KeV gamma rays which is not up to the standard needed. Furthermore, these materials have too high internal radioactivity (277 Bq/cm^3) [5] to be used in a calorimeter. There are rather recent developments of new high resolution scintillator materials. Especially the $LaBr_3(Ce)$ and $LaCl_3(Ce)$ crystals have very good energy resolution in the order of 3–4% [6,7] for 662 KeV gammas. In addition, these materials exhibit a very good light output production (63 photons/KeV and 49 photons/KeV, respectively). The internal background radioactivity is <1 Bq/cm^3. A SRIM calculation shows that detectors formed by 30 mm of $LaBr_3(Ce)$ and 150 mm of $LaCl_3(Ce)$ can in principle be used to detect protons up to 280 MeV energy with a resolution better than 2%. This combination can have enough E_γ, as well as E_p, resolution even if one takes a shorter $LaCl_3(Ce)$ crystal. As far as time response is concerned, the decay times of $LaBr_3(Ce)$ and $LaCl_3(Ce)$ are 16 ns and 28 ns, respectively [6,7], which allows for a high counting rate as well as a good energy resolution. Furthermore, the difference between the two decay times will be a key factor in the use of pulse shape analysis to separate the energy deposited in each of the two crystals. Besides the price and limited geometries available, the main drawback of these new materials is that they are extremely hygroscopic and therefore an optimum packing for a calorimeter might be difficult to achieve.

A demonstrator detector was ordered and delivered from Saint Gobain in the form of an Al cylinder of 24 mm diameter and a total length of 80 mm, with a 2-mm thick wall, containing a $LaBr_3(Ce)$ crystal of 20 mm diameter and 30 mm length coupled directly to a $LaCl_3(Ce)$ crystal of the same diameter and with 50 mm length. The cylinder is closed with a glass window of 5 mm. A Hamamatsu R5380 Photomultiplier tube (PMT) is coupled to the glass window using optical grease. The dimensions were a compromise between price and what at the time of purchase was the maximum size of $LaBr_3(Ce)$ that could be commercially obtained.

The signal from the Phoswich detector described above will consist of a superposition of two pulses, originating in light emitted from the two crystals, since a photon emitted from the $LaBr_3(Ce)$ does not correspond to the same amount of deposited energy as a photon emitted by the $LaCl_3(Ce)$. Furthermore, the decay times of the signals are different. To determine the energy absorbed in each crystal, the information in the combined pulse has to be separated into its components. The factors of proportionality between the deposited energy in each scintillator have to be determined through a calibration process. Fig. 1 illustrates what the superposed pulse along with its components may look like.

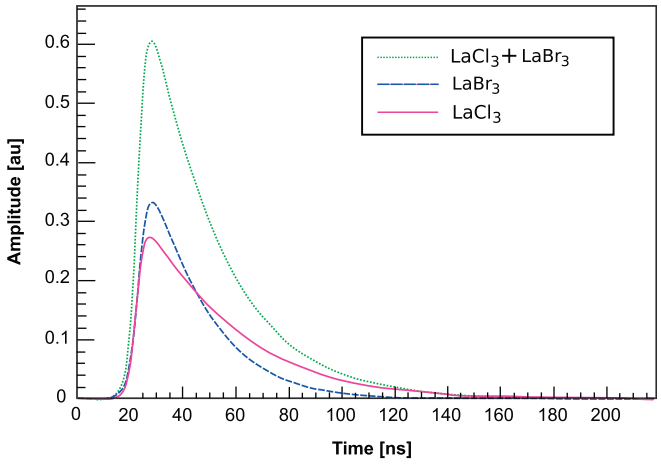

Fig. 1. Example of a superimposed pulse (dotted line) and its two components: $LaBr_3(Ce)$ (dashed line) and $LaCl_3(Ce)$ (solid line). Note the different decay times of the components.

3. Experimental test of Phoswich

3.1. Laboratory results using standard gamma sources

The Phoswich prototype was first tested in the laboratory using low-energy gamma standard sources (^{133}Ba, ^{137}Cs, ^{60}Co and ^{22}Na). The following results were obtained with the Phoswich detector mentioned above coupled to the R5380 8 stage Photo tube.

The first check was to compare the gamma response of the Phoswich to a single crystal. In Fig. 2 it is shown the energy resolution for the $LaBr_3(Ce)$ signal obtained in the case of the Phoswich compared to the ones of a separate single crystal of the same size. The relative trend with energy is clear and shows that the Phoswich combination does not deteriorate significantly the resolution, which for 662 KeV was 4.5% for the $LaBr_3(Ce)$ of the Phoswich compared to 4.4% for the individual crystal measured under identical conditions.

The main aim of the test though was to show that it is possible to distinguish the energy deposited in each of the two crystals,

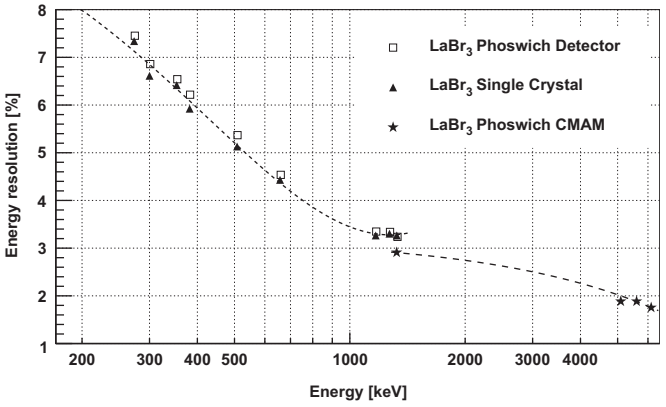

Fig. 2. The resolution of the $LaBr_3(Ce)$ response in the Phoswich compared to an individual crystal of the same shape, size and package The Phoswich assembly does not deteriorate the energy resolution of one single crystal standalone. The high energy points were taken during the CMAM experiment, see the next section.

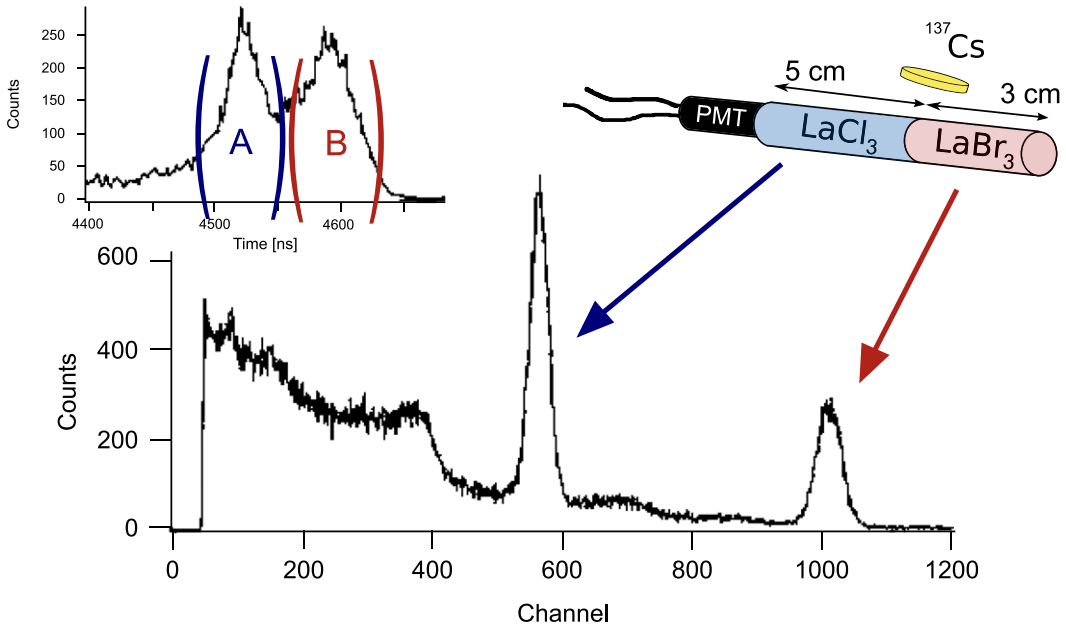

Fig. 3. The resulting energy spectrum placing a ^{137} Cs source so that it irradiates the two crystal materials simultaneously. Due to the difference in light yield by almost a factor of two, the 662 KeV gamma line shows up twice; at ch 1.000 due to the absorption in $LaBr_3$(Ce) and at ch 590 for the absorption in $LaCl_3$(Ce). The inset up left shows the time spectrum obtained passing the TFA signal via two separate CFD channels with different delays, optimized for th edecay time of $LaBr_3$(Ce) (16 ns), respectively, for the $LaCl_3$(Ce) (28 ns).

$LaBr_3$(Ce) and $LaCl_3$(Ce). For this a standard slow coincidence set-up was used where the last dynode signal of the PMT was fed to a Timing Filter Amplifier and from there to two separate Constant Fraction Discriminators (CFD) each with a different constant fraction delay. The CFD signals were further coupled as START, respectively, STOP in a Time to Amplitude Converter (TAC) and finally to a Multi Channel Analyser (MCA) in order to optimize the CF-delay for each module. Once optimized the CF-delay the threshold could be set on the TAC module and the output signal used as coincidence GATE onto the MCA. The anode signal of the PMT was sent via a preamplifier to a Spectroscopy Amplifier (Amp) and further to the MCA. It was shown possible to separate the two spectra of the two crystals in the Phoswich detector, the one from the $LaBr_3$(Ce) crystal from the one from $LaCl_3$(Ce). Fig. 3 shows the energy and time spectra obtained for a ^{137} Cs source in the position indicated in the figure. Depending on which gate (A or B) is being used the spectrum originating from the $LaBr_3$(Ce) and $LaCl_3$(Ce), respectively, could be selected. The $LaCl_3$(Ce) has about half the light-yield compared to the $LaBr_3$(Ce) and thus the photo peak in the spectrum is situated at about half in channel number in comparison to the $LaBr_3$(Ce).

3.2. Response to high energy gamma-rays

To be able to test the detector for higher energies and to test the feasibility to separate the signals in event by event mode an experiment (Fig. 4) was performed at the local 5 MV tandem accelerator at Centro de MicroAnalisis de Materiales (CMAM) [11]. A beam of 1 MeV protons and 100 pA intensity was directed onto a thick (2 cm) piece of Teflon(LiF), in order to produce gamma rays of 6129 KeV full energy together with single escape (SE), double escape (DE) and the 511 KeV, origin from the reaction $^{19}F(p,\alpha\gamma)^{16}O$.

The resulting online gamma energy spectrum from the above mentioned reaction is shown in Fig. 5. Placing a gate in the *energy vs time* spectrum, the response in each crystal could be unambiguously separated. The energy resolution obtained at 6 MeV was in the order of 1.5%.

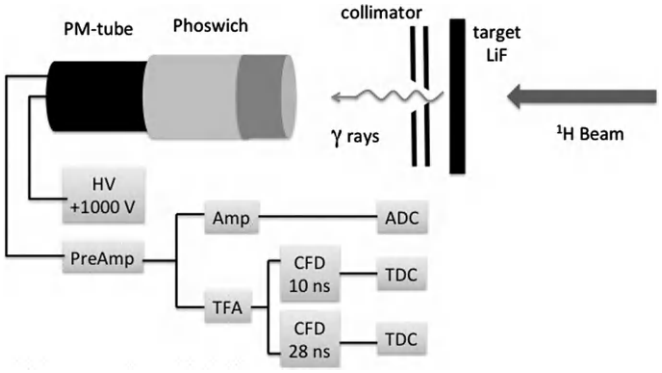

Fig. 4. To produce the high energy gamma rays (6 MeV), a 1 MeV proton beam was interacting in a thick Teflon(LiF) disc. To separate the response from the LaBr and LaCl crystals, the dynode signal of the PM-tube base was fed to a Timing Filter Amplifier (TFA) of which the output was split and fed to two Constant Fraction Discriminator (CFD) with different CFD-delays, these outputs were fed to a Time to Digital Converter (TDC). The TDC signal was used as gate signal (off-line) for the energy signal, which was fed to an Analog to Digital Converter (ADC).

3.3. Study of high energy protons at TSL Uppsala

Having shown that the assumptions made for the optical compatibility of the LaBr/LaCl Phoswich detector indeed are right and that one can, using standard NIM electronics, separate the signals, we proceed to study the direct signals from the Photo Multiplier and to record and digitize the full pulse shape in order to make off-line pulse-shape analysis.

Experimental data for protons were recorded at the The Svedberg Laboratory (TSL), Uppsala. The experiment was performed with the prototype Phoswich detector discussed above. The data consists of 10 different runs with protons of 180 MeV, 150 MeV and 120 MeV, respectively, hitting the detector in different configurations.

A low intensity proton beam at 180 MeV was provided by the Gustaf Werner Cyclotron [12] and collimated to a few millimeters.

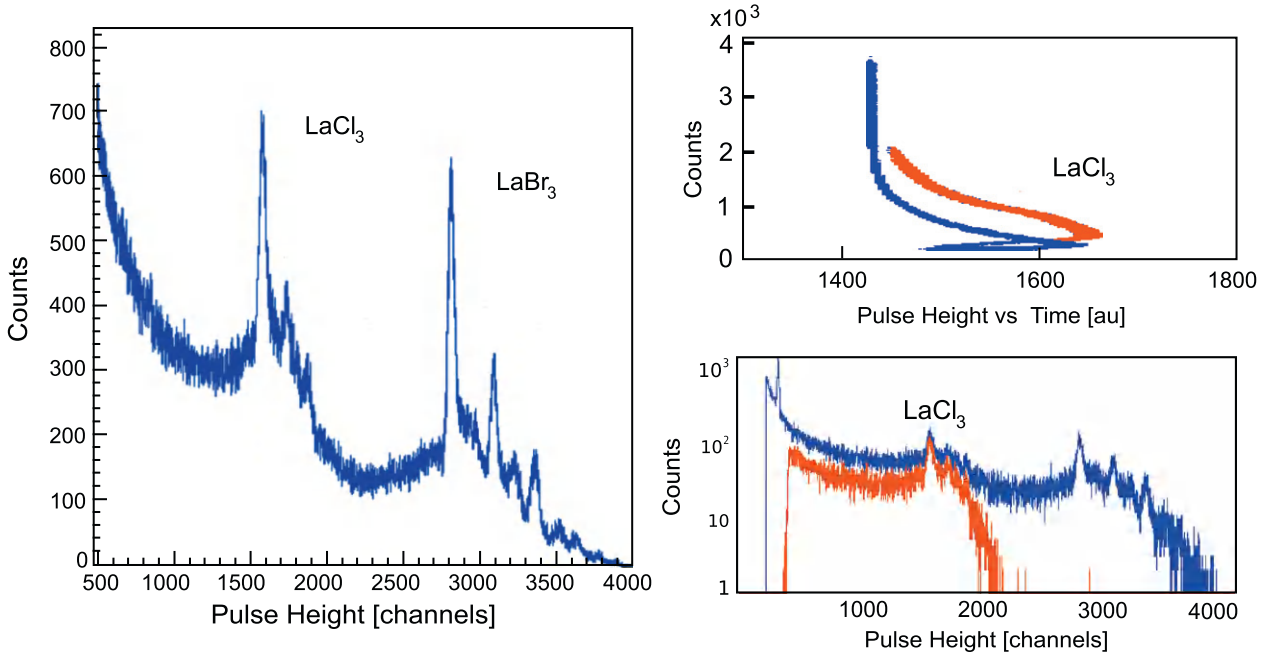

Fig. 5. The gamma energy spectrum obtained from the reaction $^{19}F(p,\alpha\gamma)^{16}O$. Placing a gate in the *energy vs time* spectrum (upper panel to right) the response in each crystal could unambiguously be separated (bottom panel).

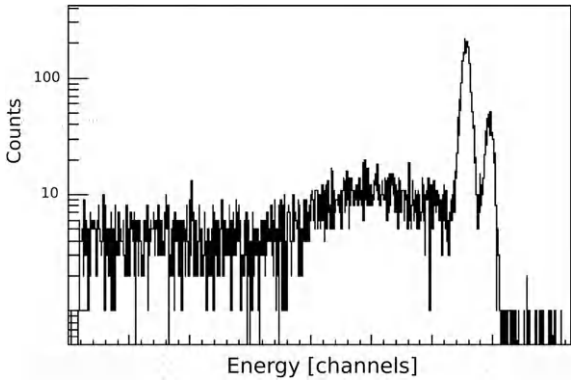

Fig. 6. The resulting energy spectrum when high energy protons of 150 and 180 MeV are impinging on the Phoswich (arbitrary log-scale) FWHM $\simeq 1\%$.

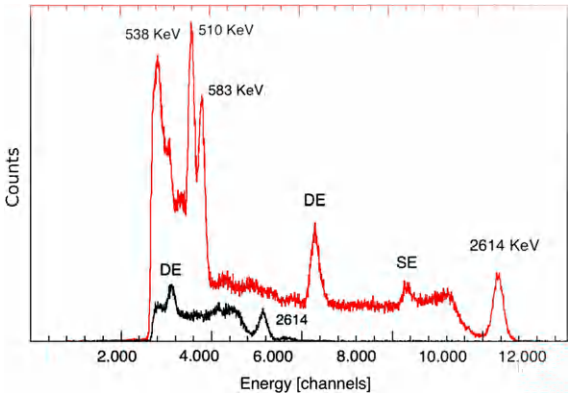

Fig. 7. The resulting energy spectrum from the daughter products from ^{228}Th-decay with the 2614 KeV gamma line from the decay of ^{208}Tl as high-energy component; main spectrum as detected in the $LaBr_3(Ce)$ with the smaller $LaCl_3(Ce)$ component shown superimposed. Both spectra were obtained with the same electronic setting as was used when detecting the high energy protons.

Degraders (20 mm of Fe, 25 mm Al) were used in order to obtain protons of lower (120 and 150 MeV) energy, respectively. The detector prototype was positioned downstream the beam line behind a Double Sided Si Strip Detector, providing position data for the incoming proton beam.

A flash ADC [13] was used to digitize the entire pulse using a 1 ns resolution for off-line analysis. The energy spectra obtained for mono energetic high energy protons of 150 and 180 MeV are shown in Fig. 6. Using the standard electronic chain with PA and Shaper gave slightly better resolution (FWHM) of $\simeq 1\%$) but showing more pile-up events that was avoided by the signal digitization and processing.

Further, the high voltage of the PMT can be adjusted in order to cover a very big dynamic range, this is especially true when using direct digitizing of the pulse where one does not have the problem of saturating an amplifier. This is illustrated by the gamma spectrum obtained from a ^{228}Th source as displayed in Fig. 7. This spectrum was obtained using the same photo tube bias voltage and electronics settings as was used for detecting the high energy (180 MeV) protons.

4. Pulse-shape Analysis

The proton data were obtained with a flash ADC recording the full pulse shape for each event. The data has been analyzed off-line in order to test different pulse-shape analysis methods. Especially two methods have proven successful; comparing the total integrated pulse to either (a) the tail or (b) the pulse height.

The analysis method is based on the pulse-shape differences between the crystals, see Fig. 1. The full integral of the digitized pulse was compared with that of the tail, as marked in Fig. 8. The full pulse was defined to start 25 ns before the peak, with endpoints in the interval of 150–300 ns after the start, whereas the tail used the same endpoint but with a varying starting point. The values will depend upon the two materials used in the Phoswich and of the energy deposition of the incoming gamma or particle. For a single crystal the ratio is a constant as is illustrated to the right in Fig. 8.

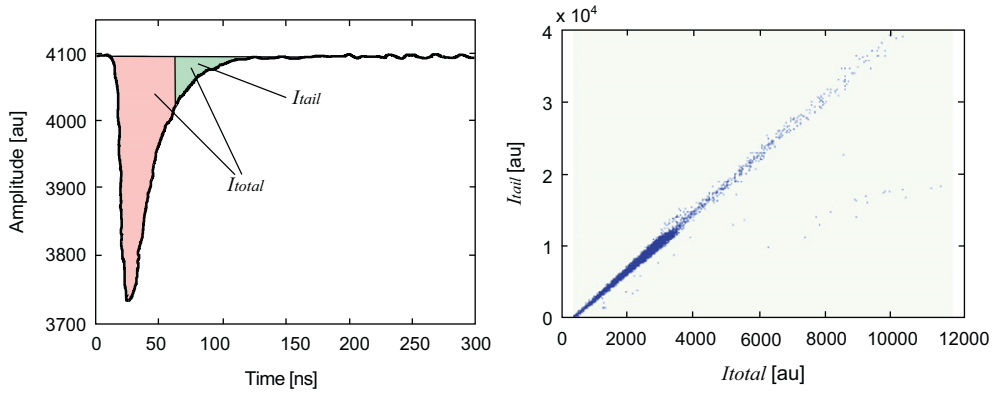

Fig. 8. To the left is illustrated how the full and tail part of the pulse are taken. To the right is plotted the obtained tail vs the full integration of each pulse, which, as seen follows a linear relation. The data shown are taken using a single $LaBr_3(Ce)$ crystal.

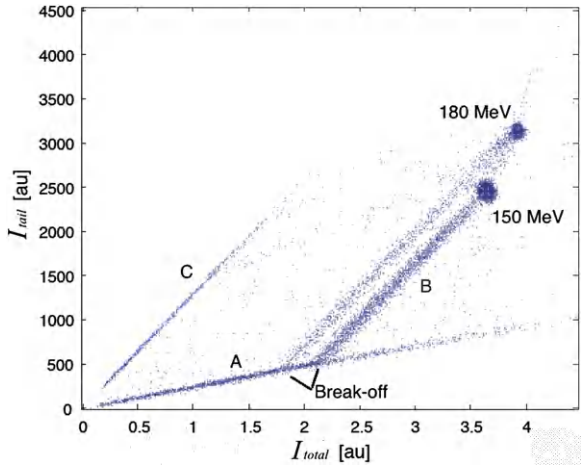

Fig. 9. The plot depicts I_{tail} vs I_{total} for the Phoswich detector when irradiated with two discrete proton energies (180 and 150 MeV). Protons depositing the full energy in the Phoswich combination, acting as a $\Delta E-E$ telescope, correspond to the two main spots. The other patterns seen in the plot all correspond to protons depositing only parts of their energy due to scattering out of or into the active volume. Scattering out of the $LaBr_3(Ce)$, leading to partial energy deposit in the first part, form line A in the plot. With increasing energy deposition, the line bifurcates at a break-off point where the maximum Bethe–Bloch energy loss in the $LaBr_3(Ce)$ is attained. The extrapolated line beyond this point corresponds to larger energy loss in the $LaBr_3(Ce)$ due to reactions in the material. Notice that the higher energy breaks out earlier as an effect of the smaller energy loss at higher energy. More details are found in the text.

When using two crystals together as a Phoswich detector the resulting plot will no longer be one single straight line, but several, as shown in Fig. 9. The slopes correspond to the different possible paths of the incoming particles and in which crystals they deposit their energy. Line A represents particles depositing their energy only in the $LaBr_3(Ce)$ and then either reacting or leaving the crystal. After the break-off point, at which line B begins, the protons have deposited energy in both crystals. Still looking at line B, only part of the energy is deposited before the proton either reacts or now leaves the second crystal. The amount of energy deposited in the $LaCl_3(Ce)$ crystal increases from the break-off point to the end of line B. The final spot of line B corresponds to events depositing all their energy in the Phoswich detector. Line C is interpreted as events scattered into the second crystal directly.

Due to the linear response with energy of the Phoswich detector, any intervals in time, gives the total pulse intensity as I combined with the intensity of the tail of the pulse is a constant factor dependent upon the material, we have

$$I = I_{Cl} + I_{Br} \quad \text{where } I_{Br}^{tail} = a_{Br} I_{Br}^{total} \text{ and } I_{Cl}^{tail} = a_{Cl} I_{Cl}^{total}$$

Combining these expressions we get

$$I_{Br}^{total} = \frac{I^{tail} - a_{Cl} \cdot I^{total}}{a_{Br} - a_{Cl}} \quad \text{and} \quad I_{Cl}^{total} = \frac{a_{Br} \cdot I^{total} - I^{tail}}{a_{Br} - a_{Cl}}$$

This enables fully the separation of the respective total pulses. In order to convert intensity into energy, a calibration factor for the amount of photons emitted per deposited energy unit in the scintillator crystal must be determined so that $I = \alpha_{xx} E$, where α is a material dependent constant, which can be obtained using data from two known energies. Thus when plotting the I^{tail} vs I^{total} for a measurement where we have two discrete proton energies line A will have two break out points depending upon the maximum energy loss of each proton energy in the first crystal, see Fig. 9. The fully absorbed protons are found in the two characteristic spots (equivalent to the, respectively, Bragg peaks). The spot with the higher integral value is interpreted as the 180 MeV protons.

The events on the slope leading up to the 180 MeV-spot could be interpreted as the line of detected protons with lower energy. This is however not correct since the events with 150 MeV are not found in a spot on this line. The detections on the line must instead be interpreted as events where particles of 180 MeV energy leave the crystal. The remaining energy in those events is lost. However, the fact that these events lie on the slope leading up to the 180 MeV tells us that they can be unambiguously assigned a total energy of 180 MeV. The same can be applied to those events which lie on the slope marked B in figure: we can assign a total energy of 150 MeV to these events even though they have deposited much less energy in the crystals. Events with a total energy of 200 MeV will be placed in a spot higher than the one of 180 MeV if fully absorbed, or in another line parallel to line B but further left in the scatter plot if part of the energy is lost. Again the assignment of 200 MeV would be unambiguous. All in all, this allows for a clean method to measure the total initial energy of the proton independently of whether they have been fully absorbed in any of the crystals or not. Note that even the protons whose energy is lost in the production of neutral particles in nuclear reactions, are assigned the correct energy. We can now go a little bit deeper in our analysis and try to parameterize the curve arising from the protons that are fully absorbed in the crystals and thus are depositing their total initial energy. This would give us an alternative method to calculate the total energy of the proton entering the detector. However, this is easier done by representing the amplitude of the signal vs its total integral as in Fig. 10. Since our experimental data consists of only two discrete proton energies (180 and 150 MeV) the curve cannot be

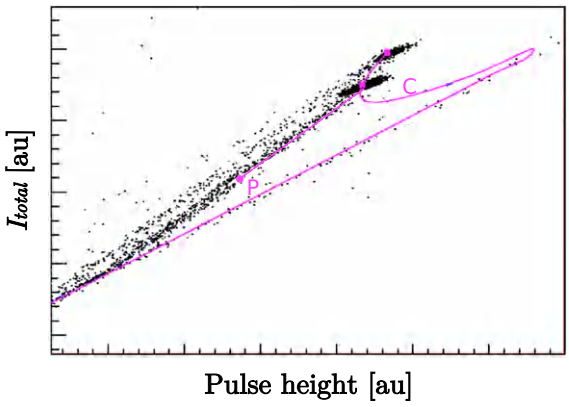

Fig. 10. Modeling the detector response with peak to amplitude, see text for explanation.

empirically established. Instead a model of the scintillators can be used and compared to the empirical values. In the most simple approximation we can estimate the amplitude of a pulse from a scintillator as an exponentially decaying function

$$A(t) = C \cdot e^{-\lambda t}$$

where λ is the decay constant, inverse of the decay time, of the scintillator and the constant C is the energy released multiplied by a proportionality constant, which will be different for different materials so that $C = a \cdot E$ where a is specific for the material and E is the deposited energy. The physical interpretation of a is what voltage will be measured (equivalent to how many photons the scintillator will give) per deposited unit of energy. For our Phoswich detector the amplitude of the signal is a superposition of two such exponential functions

$$A(t) = a_{Br} \cdot E_{Br} \cdot e^{-\lambda_{Br} t} + a_{Cl} \cdot E_{Cl} \cdot e^{-\lambda_{Cl} t}$$

This function can then be analytically integrated to

$$I(E) = \frac{a_{Br} \cdot E_{Br}^{total}}{\lambda_{Br}} + \frac{a_{Cl} \cdot E_{Cl}^{total}}{\lambda_{Cl}}$$

Modeling the maximum amplitude as the amplitude of $A(t)$ at time $t=0$ and the integral according to $I(E)$ a theoretical curve of the integral vs the amplitude can be determined. The decay constants of our scintillators are known. For an incoming particle with a given energy the range needed for the proton to deposit all of its energy can be calculated using models of the scintillator crystal. The lengths of the crystals used in our experiments are known and if the range is longer than the physical length we can determine the energy of the proton when it leaves the first crystal. The procedure is repeated for the second crystal but now with the energy left leaving the first crystal as incident energy. From this the deposited energy in each crystal can be found according with the Bethe–Bloch formula.

This leaves us with the calibration of the material specific constant a. Since we have empirical data for three specific energies we can do the range calculations for these energies and first determine how much energy will be deposited in each crystal. These energies are then compared with the empirical amplitudes and integrals. The constants a for each material can then be found by solving a linear, over-determined equation system.

Using the method described above with the simple pulse model of exponential decay yields the solid curve in Fig. 10. This method does not only reveal physical properties of the events but also provides a simple way to find the energy deposited. The easiest way to determine the energy is to find the point on curve C corresponding with the correct energy, as shown in Fig. 10 for point P.

Furthermore, this method provides a way to determine the proton energies that are higher than the actual stopping ability of the combined crystal. As seen events over 180 MeV continue on a line separate from events with lower energy. For a single crystal detector the total energy deposition curve would only be a straight line turning into itself when reaching the maximum absorption energy. Another strength of the method is the ability to determine which events are correct and which are not. According to the model only events lying on the lines in Fig. 10 can have deposited all their energy. However, events leading to reactions or events escaping the crystal can be detected and reconstructed to their real energy, detecting on which slope the event is lying.

5. Monte carlo simulations

Monte Carlo simulations of the experimental setup at Uppsala have been performed using the Geant4 simulation package [14]. The main aim of these simulations was to fine adjust the parameters of the simulation (hadronic interaction models, energy resolution, etc.) for future detector designs, as well as to completely understand the data measured and the physical processes taking place. With these ideas in mind we implemented the geometry and conditions of the experiment at TSL in full detail. The physical model for the hadronic interactions was the

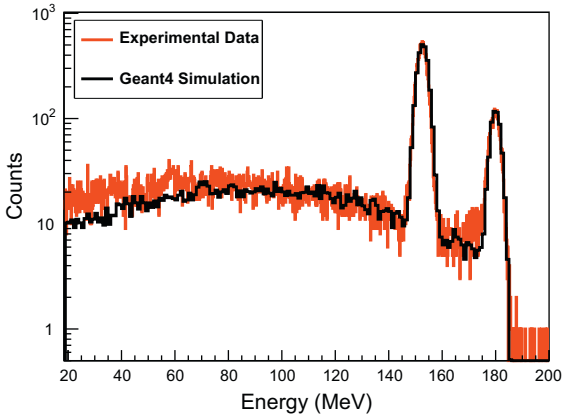

Fig. 11. Total energy deposited in the Phoswich detector. Comparison between the experimental data obtained at TSL for two proton energies (grey (online red)) and the Monte Carlo simulation (black). The energy resolution of the simulation has been adjusted so that it reproduces the measured data.

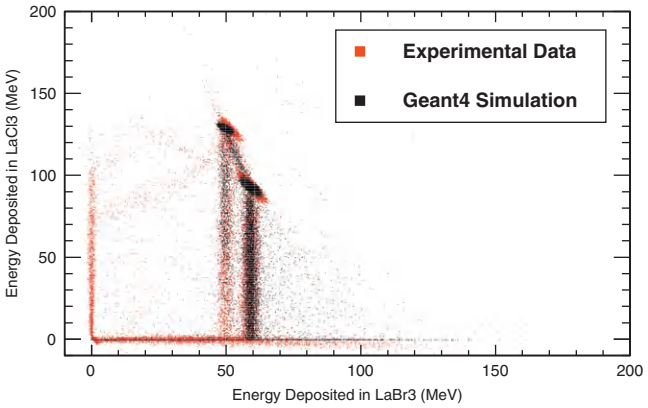

Fig. 12. Energy deposited in the $LaCl_3$ crystal vs energy deposited in the $LaBr_3$ crystal. Comparison between the experimental data obtained at TSL for two proton energies (red) and the Monte Carlo simulation (black). (For interpretation of the references to color in this figure caption, the reader is referred to the web version of this article.)

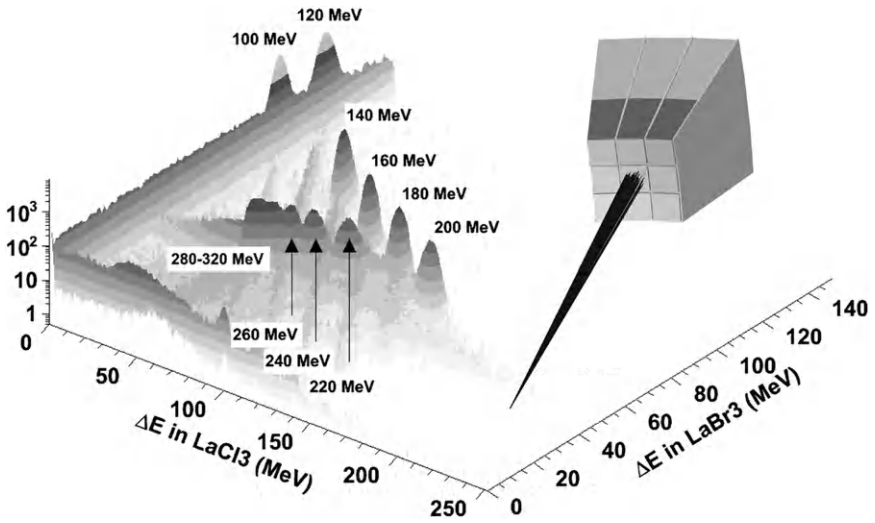

Fig. 13. Three dimensional plot showing the result of a simulation for protons between 100 and 320 MeV in steps of 20 MeV impinging in the center of an array composed by 3×3 Phoswich crystals as illustrated by the inset to the right. The energy resolution obtained from the TSL data have been used in the simulation.

Bertini Intranuclear Cascade model which has shown to work well for protons below 1 GeV [15]. As far as electromagnetic interaction is concerned, the Livermore low energy models were used when applicable to gamma-rays and electrons (for the secondary particles generated in the reactions and ionizations produced by the protons in the crystal). The energy resolution of the scintillators was adjusted to reproduce the width of the peaks of 150 MeV and 180 MeV in the proton energy spectrum as one can see in Fig. 11. In the same figure one can appreciate how well the simulation fits the experimental spectrum for both the peaks and the low energy tail due to the neutrals produced in nuclear reactions and escaping the crystal. At lowest energies the tail corresponds to the background and the simulation does not account for it so well as no source of room background or proton scattering in external volumes is included.

In order to well separate the two proton energies, one can use the Phoswich detector as a $\Delta E_1 - \Delta E_2$ telescope and plot the energy deposited in the second crystal ($LaCl_3$) vs the energy deposited in the first one ($LaBr_3$). This is shown in Fig. 12 where one can see a very clear separation of the two spots corresponding to the two proton energies. The vertical tails below the spots are due to the events that are not fully absorbed in the second crystal. Even the relative intensities of these tails are well reproduced by the Monte Carlo Geant4 simulation.

Once we have proved that the simulations work fine and reproduce quite well the experimental data, we can use the physical models and experimental resolutions previously adjusted to simulate a more complex array of Phoswich detectors. Like this, one can check the resolving power that might be achievable, with a more efficient setup, when detecting protons of higher energies that cannot be stopped by our short crystals. With this aim we have performed Monte Carlo simulations of high energy protons impinging on an array of Phoswich detectors. In this case, the lengths of the two crystals were 4 cm and 6 cm for $LaBr_3$ and $LaCl_3$, respectively. These lengths were chosen as a compromise between three different factors: the amount of nuclear reactions produced in the crystals that lead to a big escape of energy, the energy resolving power for high energy protons and the detection efficiency for gamma-rays. The shape of the crystals was that of a frustum square pyramid of side 15 mm at the entrance window and 25 mm at the exit. The array was made of 9 of these detectors stacked in a 3×3 configuration as shown in the inset of Fig. 13. The Teflon wrapping between crystals has also been included in the simulations. We call this detector CEPA. A first version of the array has already been ordered and the manufacturer is currently working on the R&D to develop the pyramidal crystals.

The results of the Monte Carlo simulation shown in Fig. 13 indicate that, with the geometry of CEPA described above, one can detect protons up to 300 MeV, with the the energy resolution at such a high energy of the order of 5%. One can get better resolution using longer crystals, but then the detection efficiency gets lower as the amount of nuclear reactions producing neutral particles increases.

6. Conclusions

A fast, high resolution Phoswich detector composed from a combination of a 3 cm long $LaBr_3$(Ce) with a 5 cm $LaCl_3$(Ce) crystal in one cylinder coupled to a Photo multiplier has been constructed and tested. It is shown that the signals from the two crystals can be separated in an *event by event* based mode both for incident gamma rays as well as for high energy protons. Using direct digitizing of the PMT pulse fed to a flash ADC a pulse-shape analysis can be performed built either on a *total to tail* or *total to pulse height* method in order to fully identify the incoming radiation. Monte Carlo simulations of the detection setup have been performed. The experimental data can be reproduced very well and this allows us to use the simulations in the design of a new Phoswich array called CEPA. This future device (currently under development) will be able to detect both gamma-rays ($E_\gamma < 30$ MeV) and protons of high energy ($E_p > 20$ MeV) with high efficiency and good energy resolution ($< 5\%$).

Acknowledgments

This work was partly financed by the Spanish Research funding agency under project CICYT FPA2007-62170, FPA2009-07387, and partly through FP7 by the Era-Net NuPNET via the project GANAS. The management of Uppsala University is acknowledged for waiving the beam-time fee at TSL.

References

[1] 〈http://www.gsi.de/GSI-Future/cdr 〉.
[2] 〈http://pro.ganil-spiral2.eu/spiral2/what-is-spiral2/physics-case/view〉.
[3] 〈http://www.gsi.de/forschung/kp/kr/R3B_e.html 〉.

[4] C.M. Pepin, et al., IEEE Transactions on Nuclear Science NS-51 (June (3)) (2004) 789.
[5] Prelude420 Data Sheet, Saint-Gobain Ceramics & Plastics, Inc., 2004.
[6] BrilLanCe 380 Data Sheet, Saint-Gobain Ceramics & Plastics, Inc., 2004.
[7] BrilLanCe 350 Data Sheet, Saint-Gobain Ceramics & Plastics, Inc., 2004.
[11] 〈http://www.cmam.uam.es/〉.
[12] The Svedberg Laboratory Uppsala 〈http://www.tsl.uu.se/〉.
[13] D. Breton, E. Delagnes, M. Houry, IEEE Transactions on Nuclear Science NS-52 (December (6)) (2005) 2853.
[14] S. Agostinelli, et al., Nuclear Instruments and Methods in Physics Research Section A 506 (2003) 250.
[15] J. Apostolakis, et al., Journal of Physics: Conference Series 160 (2009) 012073.